Archives of Hydro-Engineering and Environmental Mechanics
Vol. 54 (2007), No. 3, pp. 207–222

Drained Against Undrained Behaviour of Sand

Andrzej Sawicki, Waldemar Świdziński

Institute of Hydro-Engineering, Polish Academy of Sciences, ul. Kościerska 7, 80-328 Gdańsk, Poland,
e-mails: as@ibwpan.gda.pl, waldek@ibwpan.gda.pl

(Received September 11, 2007; revised October 26, 2007)

Abstract

The incremental constitutive equations describing the pre-failure deformations of sand are presented. These equations were calibrated on the basis of extensive experimental data, obtained from investigations performed in a triaxial apparatus. Incremental equations were calibrated separately for initially contractive and dilative soil samples. Then, they were applied to predict the undrained behaviour of saturated soil samples. In the case of contractive soils, the constitutive equations describe the effective stress paths leading to the static liquefaction. In the case of dilative soils, the effective stress path is different, as the mean effective stress initially decreases, and after passing the instability line, it starts to increase, asymptotically reaching the failure envelope. Theoretical predictions of undrained behaviour are supported by experimental data. The original feature of this paper is that one can predict the undrained behaviour of saturated granular soils on the basis of stress-strain characteristics of the same soil but dry or tested in drained conditions.

Key words: granular soils, stress-strain characteristics, instability line, dilative and contractive behaviour, static liquefaction

1. Introduction

The mechanical behaviour of granular soils differs essentially from that of other materials, mainly due to specific volumetric strains that develop during shearing. Experimental results show that some granular soils compact when sheared, and some dilate, depending on their initial state. In traditional soil mechanics, the initial state of granular soil is characterized by a single parameter, defined as the void ratio e, see Craig (1987), Atkinson (1993). More recent experimental investigations have revealed that the initial state of granular soils should rather be defined by a pair of parameters, namely: e and p' = mean effective stress, see Poulos (1981). It was also found that, in the plane $\log p' - e$, there exists a straight line corresponding to the **steady state** of granular soil (SSL).

The steady state corresponds to continuous deformation of soil, at constant volume and constant stresses (Castro 1975, Poulos 1981). The region above SSL corresponds to the **contractive** behaviour of soil, which means that this soil, when

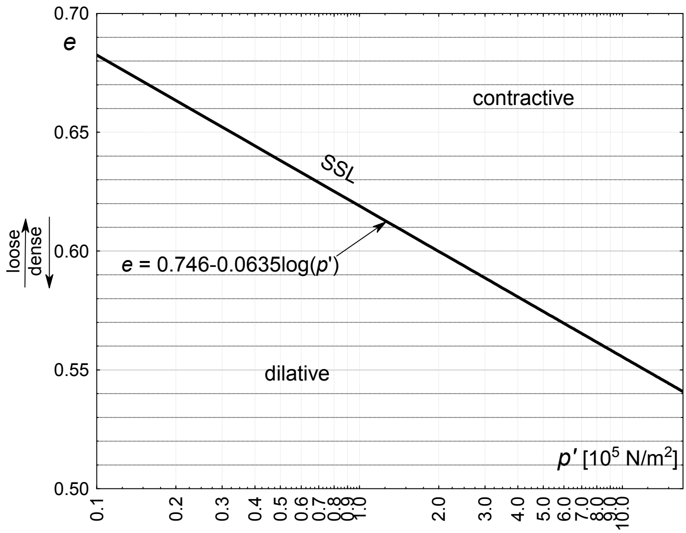

Fig. 1. Steady state line (SSL) for "Skarpa" sand separating the contractive and dilative regions

dry or in free drainage conditions, densifies during shearing. The region below SSL corresponds to the dilative behaviour, when the soil dilates during shearing (volumetric expansion), see Fig. 1.

The distinction between the contractive and dilative states is important in modelling the pre-failure stress strain behaviour of granular soils, both dry and water saturated, as this behaviour strongly depends on the initial state of the soil sample. In order to study these behaviours, the extensive experimental programme has been carried out in the Institute of Hydro-Engineering for many years, see Świdziński and Mierczyński (2002, 2005) and Świdziński (2006). The experiments were performed in a computer controlled triaxial testing system manufactured by GDS Instruments, see Menzies (1988). This system enables the local measurement of both lateral and vertical strains. The experiments were performed on the model quartz sand "Skarpa", characterized by the following parameters: maximum void ratio $e_{\max} = 0.677$, minimum void ratio $e_{\min} = 0.423$; angles of internal friction $\phi = 34°$ (loose sand) and $\phi = 41°$ (dense sand), determined from triaxial compression tests. Summary of the most important experimental results will be presented in subsequent sections.

The aim of this paper is to show how the undrained behaviour of saturated granular soils can be predicted from the stress-strain relations derived for the same soil, but tested in dry or drained conditions. First, the incremental equations describing the stress-strain behaviour of dry/drained sand are summarized, after Sawicki (2007). These equations have different forms for initially contractive and dilative sand. In the case of dilative soil, the existence of instability line is taken into account in the incremental equations.

Then, these incremental equations, describing the pre-failure deformations of sand, are applied to predict the undrained behaviour of saturated samples. In the case of contractive soil, the predicted effective stress path is similar to that observed in experiments. The stress deviator reaches its maximum value in the vicinity of the instability line, and then decreases. The mean effective stress continuously decreases due to the pore-pressure generation, and the effective stress path approaches the failure envelope, finally reaching almost zero effective stresses. Such a phenomenon is known as the so-called static liquefaction. In the case of dilative soils, the effective stress path is different. Before reaching the instability line, the mean effective stress decreases, and then begins to increase. The stress path eventually approaches the failure surface or not, but in the opposite direction in comparison with the contractive soil. This behaviour corresponds to the initial generation of pore-pressure, and then its subsequent decrease. The predicted behaviour is supported again by experimental data.

The original and useful features of the present paper are the following:

– the links between the drained and undrained behaviours of granular soils are shown in the explicit form,
– the equations governing the soil behaviour take into account the initially contractive or dilative state of the soil, as well as the instability line,
– a summary of an extensive experimental programme is presented, which may be useful for other researchers.

2. Drained Behaviour

2.1. Basic Definitions

In this Section, the summary of basic stress-strain characteristics of "Skarpa" sand, tested in either dry or free draining conditions, are presented. They are related to loading and unloading along simple stress paths, shown in Fig. 2, for the configuration of triaxial tests.

The following notation is used in this paper:

$$p' = \frac{1}{3}\left(\sigma_1' + 2\sigma_3'\right), \tag{1}$$

$$q = \sigma_1' - \sigma_3' = \sigma_1 - \sigma_3, \tag{2}$$

$$\varepsilon_v = \varepsilon_1 + 2\varepsilon_3, \tag{3}$$

$$\varepsilon_q = \frac{2}{3}\left(\varepsilon_1 - \varepsilon_3\right), \tag{4}$$

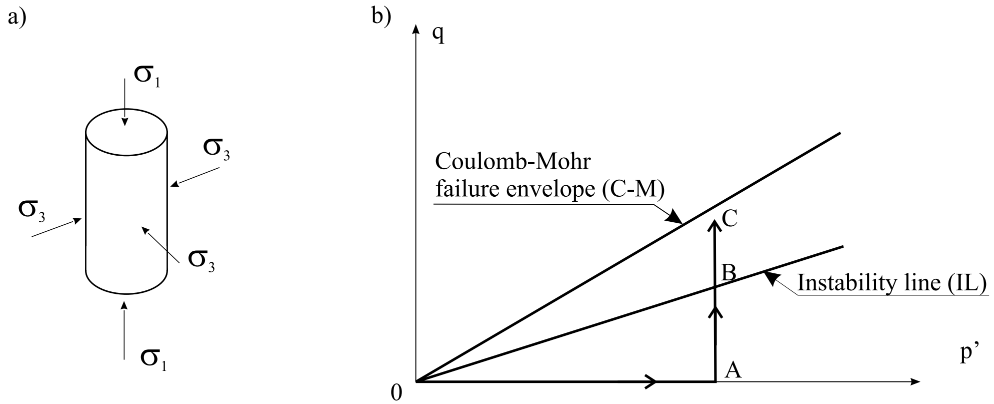

Fig. 2. Soil sample in triaxial apparatus (a); simple stress paths applied for determination of deformation characteristics (b)

where: σ_1 = vertical total stress; $\sigma'_1 = \sigma_1 - u$ = vertical effective stress, σ_3 = horizontal total stress; $\sigma'_3 = \sigma_3 - u$ = horizontal effective stress; u = pore pressure; ε_1 = vertical strain; ε_3 = horizontal strain. For dry or free draining conditions: $\sigma'_1 = \sigma_1$ and $\sigma'_3 = \sigma_3$, as $u = 0$ in this case. The quantities appearing in Eqs. (1) to (4) are designated as follows: p' = mean effective stress, q = stress deviator; ε_v = volumetric strain; ε_q = deviatoric strain. The soil mechanics sign convention is used, where the plus sign denotes compression. The following definition of loading and unloading is accepted:

- spherical loading when $dp' > 0$;
- spherical unloading when $dp' < 0$;
- deviatoric loading when $dq > 0$;
- deviatoric unloading when $dq < 0$.

The above definition of loading/unloading is related to the simple stress paths shown in Fig. 2b, which is sufficient for the present purposes. In general, the problem of loading and unloading is more complex, see Życzkowski (1973). Some additional aspects of this problem are discussed in the next Section, in connection with the undrained behaviour of granular soils.

2.2. Stress-Strain Curves

Figs. 3 to 5 illustrate typical stress-strain characteristics of "Skarpa" sand, related to the stress paths shown in Fig. 2b, after Sawicki (2007). The strains that develop during isotropic compression (path OA in Fig. 2b) are presented in Fig. 3. A qualitative character of these stress-strain curves is similar for both dilative and contractive soils.

An interesting feature of this behaviour is that the deviatoric strains develop during the isotropic compression, which means that the samples investigated display

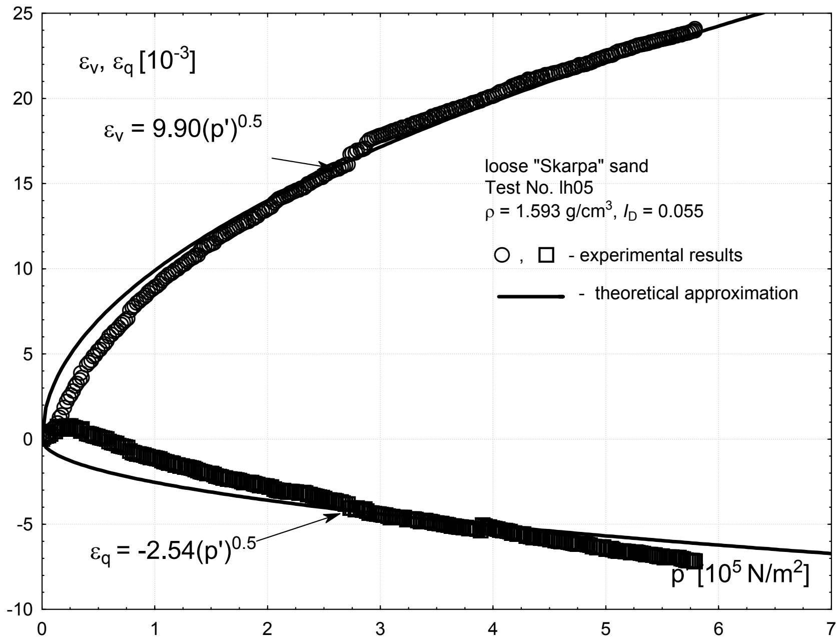

Fig. 3. Volumetric and deviatoric strains developing during isotropic compression of dry/drained sand (stress path OA in Fig. 2b)

an anisotropic character, in spite of very careful preparation of these samples in order to obtain initially isotropic sand.

Fig. 4 shows the volumetric changes due to pure shearing (path ABC in Fig. 2b) of two samples of "Skarpa" sand characterized by initially contractive and dilative state, see Fig. 1. Note that there is a new variable $\eta = q/p'$ on the horizontal axis, and also a new variable $\varepsilon_v/\sqrt{p'}$ on the vertical axis. These variables were introduced in order to present results of different experiments, performed for various values of p', in a common plot.

A basic difference between contractive and dilative samples is that the initially contractive soil densifies during pure shearing, whilst the dilative soil first densifies and then dilates. The maximum densification of dilative soil corresponds to $\eta = \eta'$, which is identified with the instability line, see Fig. 2b. Extreme values of volumetric strains correspond to the failure envelope $\eta = \eta''$. Note that the volumetric strains reach finite value for $\eta = \eta''$, which means that it is not an asymptotic behaviour! During the unloading corresponding to $d\eta < 0$, which is equivalent to $dq < 0$ (p' = const in each experiment), the sand densifies in both cases. The stress-strain characteristics were found to be almost linear.

Fig. 5 shows the shape of the deviatoric strain-stress curve during pure shearing (path ABCBA in Fig. 2b). This shape is similar for both contractive and dilative soils.

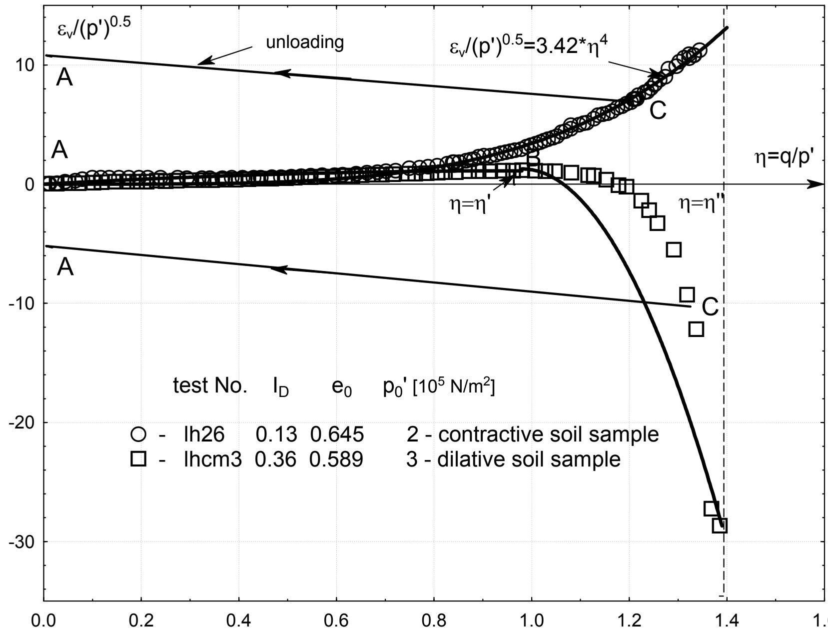

Fig. 4. Volumetric changes due to pure shearing of contractive and dilative sand samples

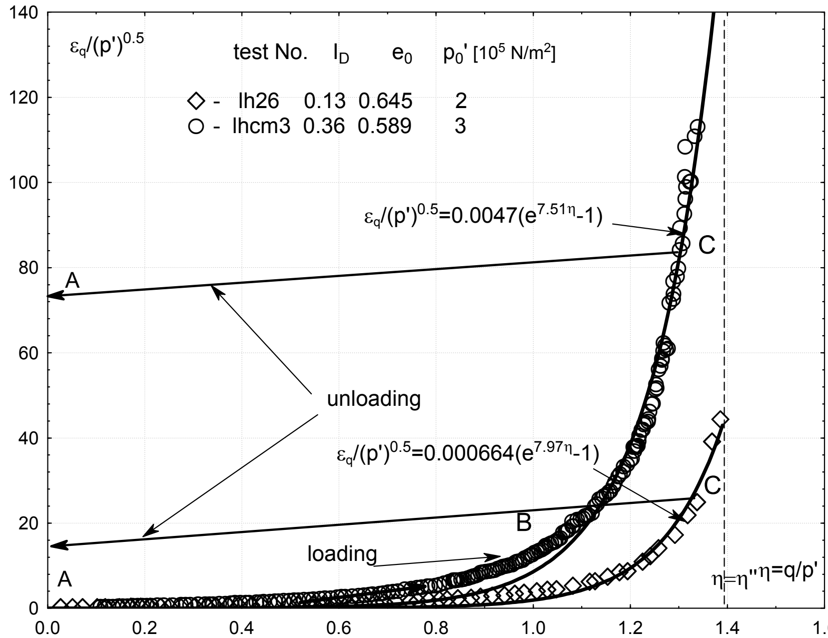

Fig. 5. Deviatoric deformations due to pure shearing. The qualitative behaviour of contractive and dilative soils is similar

2.3. Incremental Equations

It is assumed that the following incremental equations describe the pre-failure deformations of granular soils:

$$d\varepsilon_v = Mdp' + Ndq, \tag{5}$$

$$d\varepsilon_q = Pdp' + Qdq, \tag{6}$$

where M, N, P, Q are certain functions, which should be determined from basic experimental results presented in the previous section. These functions are different for dilative and contractive soils, and also have different shapes for loading and unloading. Tables 1 and 2 summarize these functions, after Sawicki (2007).

Table 1. Functions appearing in Eqs. (5) and (6) for contractive soil

Function	loading	unloading
M	$\dfrac{A_v}{2\sqrt{p'}}$	$\dfrac{A_v^u}{2\sqrt{p'}}$
N	$\dfrac{4c_1\eta^3}{\sqrt{p'}}$	$\dfrac{a_v^c}{\sqrt{p'}}$
P	$\dfrac{A_q}{2\sqrt{p'}}$	$\dfrac{A_q^u}{2\sqrt{p'}}$
Q	$\dfrac{g_1 g_2}{\sqrt{p'}}\exp(g_2\eta)$	$\dfrac{g_q}{\sqrt{p'}}$

Table 2. Functions appearing in Eqs. (5) and (6) for dilative soil

Function	loading	unloading
M	$\dfrac{A_v}{2\sqrt{p'}}$	$\dfrac{A_v^u}{2\sqrt{p'}}$
N	$\dfrac{1}{\sqrt{p'}}(2a_1\eta + a_2)\,; 0 \le \eta \le \eta'$ $\dfrac{1}{\sqrt{p'}}(2a_3\eta + a_4)\,; \eta' \le \eta \le \eta''$	$\dfrac{a_v^d}{\sqrt{p'}}$
P	$\dfrac{A_q}{2\sqrt{p'}}$	$\dfrac{A_q^u}{2\sqrt{p'}}$
Q	$\dfrac{b_1 b_2}{\sqrt{p'}}\exp(b_2\eta)$	$\dfrac{b_q}{\sqrt{p'}}$

The following parameters appear in functions M, N, P, Q: A_v; A_v^u; c_1; a_v^c; A_q; A_q^u; g_1; g_2; g_q; a_1; a_2; a_3; a_4; a_v^d; b_1; b_2; b_q. Altogether, there are 17 parameters, but note that their number will increase as, for example the parameters A_v, A_q take different values for initially loose and dense soils. Also note, that there are some additional parameters as, for example, η' and η'' which characterize particular soil.

2.4. About Soil Parameters

Such a large number of parameters, as that introduced in Section 2.3, is of little practical importance, because their experimental determination would be expensive and time consuming. However, in this paper, we are not attempting to propose a practically useful model, but we would like to investigate the real behaviour of actual soil. Models containing "the minimal set of material parameters" usually lead to predictions which do not conform with experimental data. For example, we have attempted to describe our rich empirical database using well known models of soils, but with little success, see Sawicki (2003), Głębowicz (2006). It seems that experience of other authors is similar, cf. Saada and Bianchini (1987), Kolymbas (2000).

Eqs. (5) and (6), with functions presented in Tables 1 and 2, describe very well the mean results of tens of experiments performed in the laboratory of the Institute of Hydro-Engineering. They have been derived empirically, as a result of analysis of rough experimental data. Therefore, they can also be useful for theoretical modellers. Below, numerical values of the introduced coefficients, corresponding to "Skarpa" sand, are presented.

The coefficients presented are expressed in **useful units**, namely **stress unit 10^5 N/m^2** and **strains unit 10^{-3}**. The reason for choosing such units is purely practical, as in numerical calculations we can deal with numbers of a similar order of magnitude. For example, if q = 200 kPa = 2 × 10^5 N/m^2, we introduce into the respective equation just 2. If, after integration of Eq. (6), we obtain ε_q = 0.5 (expressed in strain unit) it means that the real strain is 0.5 × 10^{-3} (see also Section 2.5).

Table 3. Average parameters describing isotropic compression of "Skarpa" sand, after Sawicki (2007)

Initial I_D	A_v	A_v^u	A_q	A_q^u
Loose 0.02–0.44	6.01	4.41	–0.905	–0.047
Dense 0.71–0.86	3.47	2.91	–0.470	–0.205

Table 3 shows the average parameters describing isotropic compression of "Skarpa" sand. The other parameters, appearing in functions M, N, P, Q, are the following:
$c_1 = 3.4$; $a_v^c = -0.87$; $g_1 = 0.0206$; $g_2 = 4.587$; $g_q = 0.76$; $a_1 = -1.458$; $a_2 = 2.39$; $a_3 = -42.215$; $a_4 = 69.232$; $a_v^d = -0.386$; $b_1 = 2.67 \times 10^{-3}$; $b_2 = 5.248$; $b_q = 0.4$.

2.5. Example

Consider the isotropic loading (stress path OA in Fig. 2b) of initially loose and dry "Skarpa" sand. Determine the strains that develop during this loading.

Because $dq = 0$, Eqs. (5) and (6) take the following form, after introducing respective expressions from Table 1 (or Table 2 which does not make a difference, as respective equations are similar for both contractive and dilative soils in this case):

$$d\varepsilon_v = \frac{A_v}{2\sqrt{p'}}dp'; \quad d\varepsilon_q = \frac{A_q}{2\sqrt{p'}}dp'. \tag{7}$$

Integration of these equations, with zero initial conditions, gives the following stress-strain relations (see Fig. 3):

$$\varepsilon_v = A_v\sqrt{p'}; \quad \varepsilon_q = A_q\sqrt{p'}, \tag{8}$$

where $A_v = 6.01$ and $A_q = -0.905$ (see Table 3).

For example, the volumetric strain for $p' = 2 \times 10^5$ N/m^2 can be calculated as follows: $\varepsilon_v = 6.01\sqrt{2} = 8.5$, which means that the real strain is $8.5 \times 10^{-3} = 0.0085$.

3. Undrained Behaviour

3.1. Basic Relations

Granular soils as, for example, sands, are permeable, but when duration of loading is short enough to prevent dissipation of excess pore-pressure, their behaviour can be approximated assuming undrained conditions, as in the case of impulse loads or earthquake shaking. The assumption of undrained behaviour means that the volumetric deformation of saturated soil is zero, if the pore water is incompressible (i.e. does not contain gas). It follows from Eq. (5) that in this case:

$$Mdp' + Ndq = 0, \tag{9}$$

where $dp' = dp - du$.

Therefore:

$$du = dp + \frac{N}{M}dq. \tag{10}$$

Eq. (10) can be integrated for the given history of loading, and respective history of pore-pressure changes determined.

In the case of compressible pore fluid, i.e. when it contains some admixture of gas, Eq. (9) is invalid as the global volumetric deformation of saturated soil will depend on the compressibility of pore-fluid, assuming that the solid grains are incompressible.

Consider the volume V_0 of saturated sand before deformation, which reduces to V after volumetric deformation. The volumetric strain is defined traditionally as:

$$\varepsilon_v = \frac{V_0 - V}{V_0}. \tag{11}$$

The volume V_0 consists of two parts:

$$V_0 = V_0^f + V_0^g, \tag{12}$$

where V_0^f = initial volume of pore fluid, $V_0^g = V^g$ = volume of grains. It follows from Eqs. (11) and (12) that:

$$\varepsilon_v = \frac{V_0^f - V^f}{V_0} = \frac{V_0^f - V^f}{V_0^f}\frac{V_0^f}{V_0} = \chi_f u n_0, \tag{13}$$

where χ_f = pore fluid compressibility; n_0 = initial porosity. Therefore, in undrained conditions, we have:

$$\chi_f n_0 du = Mdp' + Ndq, \tag{14}$$

and after simple manipulations:

$$du = \frac{1}{M + n_0\chi_f}(Mdp + Ndq). \tag{15}$$

For incompressible pore fluid ($\chi_f = 0$), Eq. (15) reduces to Eq. (10). Having known the pore pressure changes for given history of total stresses p and q, one can determine respective changes of the mean stress p', and subsequently the undrained behaviour of saturated granular soil. In the next sections, such a behaviour will be analysed in detail, separately for initially contractive and dilative soils.

3.2. Loading and Unloading

The basic definitions of loading and unloading were introduced in Section 2.1, in connection with interpretation of experimental data. In Section 2.2, we have also introduced a new variable $\eta = q/p'$, which has been found useful in presentation of the stress-strain curves shown in Figs. 4 and 5. These figures correspond to experiments performed at p' = const which means that for $dq > 0$(loading) there is also $d\eta > 0$. In undrained conditions, both stress variables, i.e. q and p', change, so there is a need to define the deviatoric loading and unloading more precisely.

Recall that in the case of p' = const, η increases when q increases. In the case q = const, η increases when p' decreases, which means that deviatoric deformations are possible when the stress deviator does not changes (not to mention deviatoric changes due to initial anisotropic structure of the soil). In the case when q increases and p' decreases, the new variable η also increases. Consider now an interesting case when both q and p' increase. The increment of η is given by the following formula:

$$d\eta = \frac{\partial \eta}{\partial p'} dp' + \frac{\partial \eta}{\partial q} dq = \frac{1}{p'} \left(dq - \eta dp' \right). \tag{16}$$

Therefore, for deviatoric loading we have:

$$d\eta = \frac{1}{p'} \left(dq - \eta dp' \right) > 0, \tag{17}$$

or

$$dq - \eta dp' > 0 \tag{18}$$

as $p' > 0$ for granular soils.

In the case of unloading, there is:

$$dq - \eta dp' < 0. \tag{19}$$

The relations (18) and (19) can be illustrated graphically in the stress space, as shown in Fig. 6. The stress increments directed upwards the line η = const correspond to deviatoric loading. There is obviously $d\eta > 0$ in this case, as these stress increments define a new line $\eta + d\eta$ = const. The other stress increments correspond to unloading.

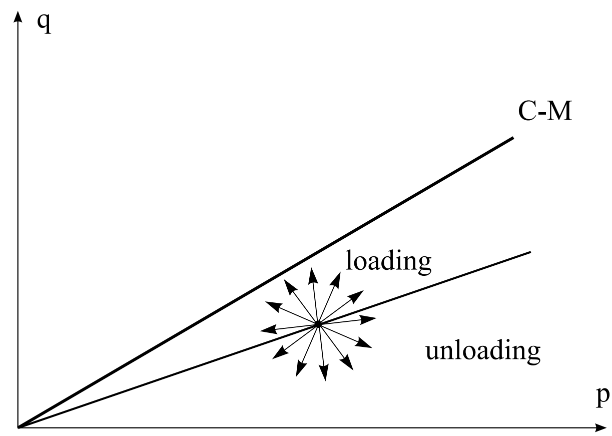

Fig. 6. Stress increments above the line η = const define deviatoric loading. Unloading corresponds to stress increments directed below the line η = const

The conditions (18) and (19) should be checked when integrating Eqs. (10) and (15), as the choice of function N depends on the type of loading.

3.3. Static Liquefaction of Contractive Soil

Eq. (9) presents the condition of undrained behaviour expressed in terms of independent variables p' and q. Sometimes, it is more convenient to apply the other pair of independent variables, p' and η. Note that the function N (see Table 1) was derived from the shape of respective curve shown in Fig. 4:

$$\varepsilon_v^q = c_1 \sqrt{p'}\eta^4, \tag{20}$$

where the superscript q distinguishes the volumetric strain caused by shearing.

Note that during shearing of the soil sample in undrained conditions the mean effective stress changes, in contrast to conditions kept during experiments with full drainage, when p' was kept constant. Therefore, the total differential of volumetric strain is the following:

$$d\varepsilon_v = \frac{\partial \varepsilon_v^q}{\partial p'} dp' + \frac{\partial \varepsilon_v^q}{\partial \eta} d\eta + \frac{A_v^u}{2\sqrt{p'}} dp' = 0. \tag{21}$$

Note that the third term in the above expression represents the volumetric change due to spherical unloading. Eqs. (20) and (21) lead to the following differential equation, describing the changes of mean effective stress during undrained shearing:

$$\frac{dp'}{p'} = -\frac{6\eta^3}{\eta^4 + \dfrac{A_v^u}{c_1}} d\eta. \tag{22}$$

Integration of this equation, with the initial condition: $p' = p_0$ for $\eta = 0$; p_0 = initial confining stress, leads to the following formula:

$$p' = p_0 \left[\frac{1}{1 + \dfrac{c_1}{A_v^u}\eta^4} \right]^{3/2}. \tag{23}$$

Fig. 7 shows the stress path calculated from Eq. (23) for the following data: c_1 = 3.4; A_v^u = 4.4; p_0 = 2 against the experimental results obtained by Świdziński and Mierczyński (2005). It can be seen that for these values the predicted curve does not reproduce the experimental data too well (solid line), however after some small corrections of the values of c_1 and A_v^u coefficients the conformity is much better (dashed line).

Note that the model presented in this paper correctly predicts the undrained behaviour of contractive soil during shearing. Calculations are terminated on the Coulomb-Mohr yield surface which corresponds to the so-called "static liquefaction".

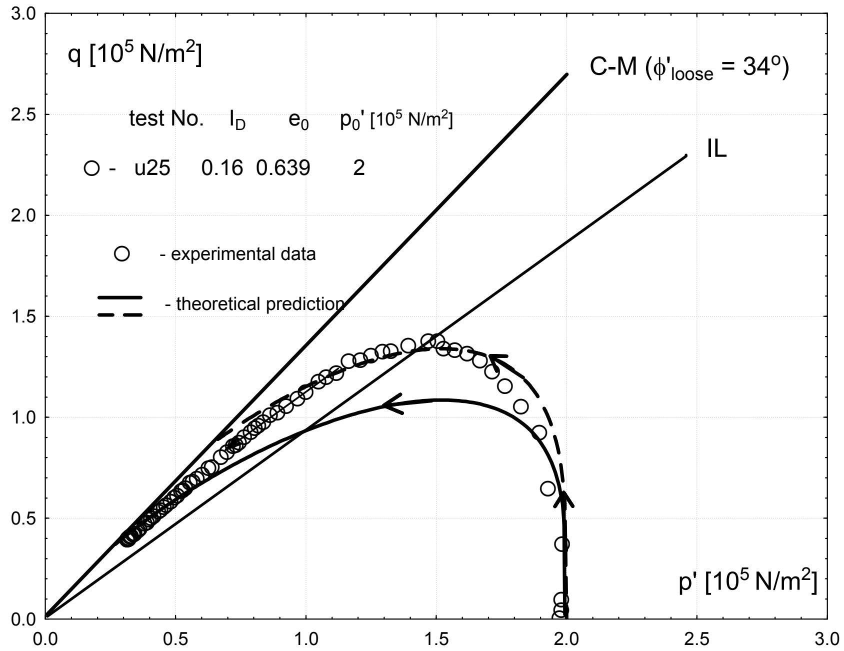

Fig. 7. Experimental and predicted stress paths during undrained shearing of saturated contractive soil

Quantitative analysis of this result shows that the maximum value of stress deviator q corresponds to $\eta \approx 0.7$, whilst the instability line in drained tests corresponds to η lying in the interval (0.9–1). Note that the volumetric strain curves, shown in Figs. 3 and 4 (contractive soil), do not contain any features indicating that the instability line exists. This feature is visible only when these curves are applied to predict the undrained shearing of contractive soil, see Fig. 7.

3.4. Undrained Behaviour of Dilative Soil

The volumetric strains of drained dilative soil due to shearing are shown in Fig. 4. In this case, they can be described by the incremental equation (5), with respective functions listed in Table 2. Then, a similar procedure to that described previously can be applied to study the undrained behaviour. However, such a procedure, applied to the functions mentioned, does not lead to simple formulae describing the effective stress paths in undrained conditions, although there is no problem with numerical integration of such equations. In order to simplify the analysis of undrained shearing, and to obtain analytical formulae for the effective stress paths, a bi-linear approximation of respective deviatoric stress – volumetric strain is applied in this section, see Fig. 8.

The AB part of the stress-strain curve can be approximated by the following simple formula:

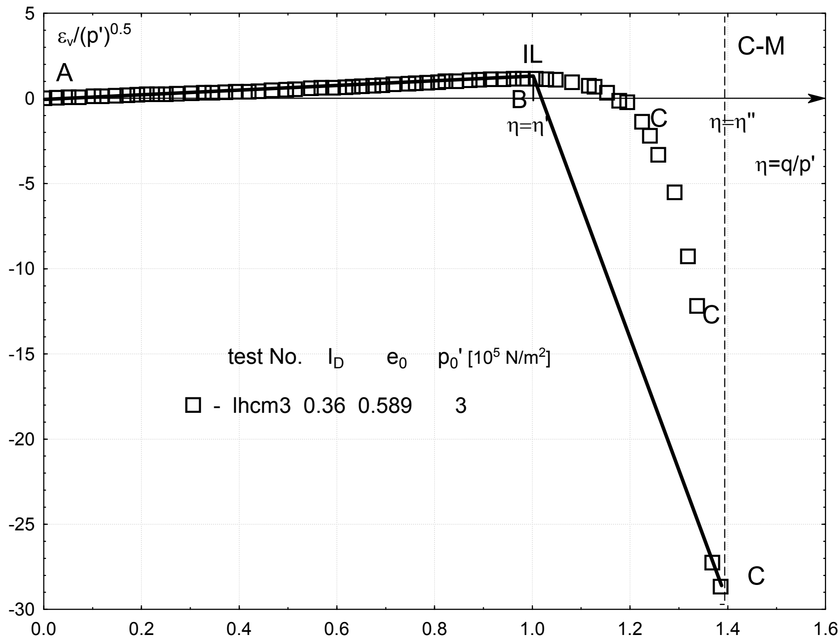

Fig. 8. Bi-linear approximation of the deviatoric stress-volumetric strain curve for dilative soil, cf. Fig. 4

$$\frac{\varepsilon_v^q}{\sqrt{p'}} = B_v\eta, \tag{24}$$

where $B_v = 1.195$ in the case considered (recall respective units!). Already known procedure leads to the following relation:

$$d\varepsilon_v = \frac{1}{2\sqrt{p'}}[B_v\eta + A_v^u]dp' + \sqrt{p'}B_v d\eta = 0. \tag{25}$$

Integration of this equation leads to the following analytical formula, valid for $\eta \in < 0, \eta' >$, where η' corresponds to the instability line:

$$p' = p_0 \frac{1}{\left(1 + \dfrac{B_v}{A_v^u}\eta\right)^2}. \tag{26}$$

In the interval BC, we have:

$$\frac{\varepsilon_v^q}{\sqrt{p'}} = C_v\eta + D_v, \tag{27}$$

and similar procedure leads to the following analytical solution:

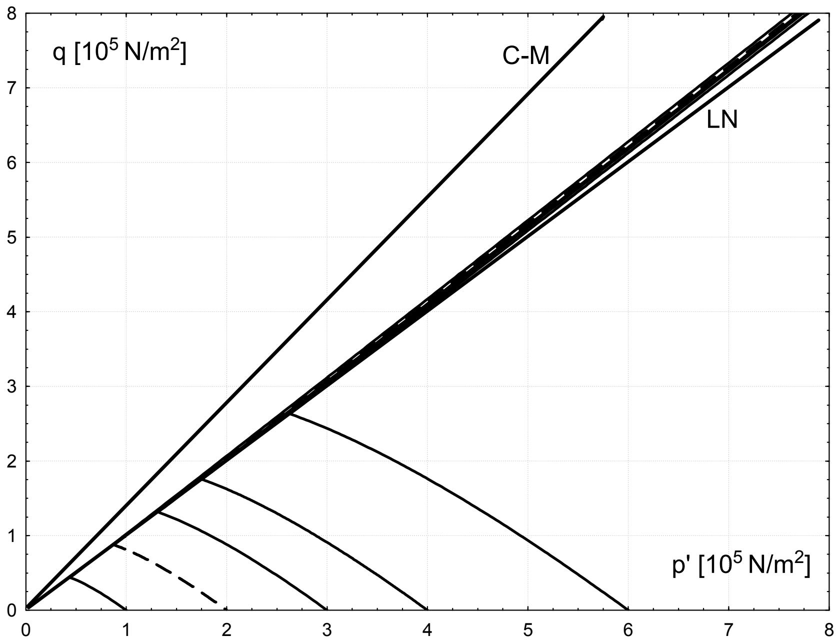

Fig. 9. Predicted effective stress path during undrained shearing of dilative "Skarpa" sand

$$p' = p^* \left(\frac{\eta' + \xi}{\eta + \xi} \right)^2, \tag{28}$$

where $\xi = (D_v + A_v)/C_v$, and p^* corresponds to the mean effective stress on the instability line, and η' corresponds to the instability line (point B in Fig. 8). Eqs. (26) and (28) define the effective stress paths, corresponding to undrained shearing of dilative soil.

Example: Assume the following data that correspond to the dilative "Skarpa" sand: $A_v = 3.47$; $A_v^u = 2.91$; $B_v = 1.486$; $C_v = -77.79$; $D_v = 79.256$; $\eta' = 1.0$; $\eta'' = 1.395$; $p_0 = 2$. Fig. 9 illustrates the stress paths calculated for the above data (dashed line). It is similar to that of contractive soil before reaching the instability line. In the same figure some other stress paths, calculated for other initial mean effective stresses, have also been shown reflecting well the qualitative character of experimental results.

4. Conclusions

The main results presented in this paper can be summarized as follows:

A) The summary of experimental results dealing with the pre-failure behaviour of granular soils are presented. These results represent the volumetric and deviatoric strains of initially contractive or dilative soils, subjected to simple stress paths in dry or fully drained conditions. The empirical results presented are then approximated by simple mathematical formulae, which can be used by other researchers to validate their models.

B) The stress-strain curves, corresponding to drained conditions, are applied to predict the effective stress paths for undrained conditions. It was shown that the drained stress-strain characteristics lead to prediction of so-called static liquefaction in the case of contractive soil, in accordance with experimental data. In the case of dilative soil, the predicted behaviour is also consistent with experimental results.

C) The role of instability line is also discussed in this paper.

Acknowledgement

Research presented in this paper was supported by the Polish Ministry of Science and Higher Education: research grant No. 4 T07A 028 30. We greatly appreciate this generous support.

References

Atkinson J. H. (1993) *An Introduction to the Mechanics of Soil and Foundations*, McGraw-Hill, London.

Castro G. (1975) Liquefaction and cyclic mobility of saturated sands, *J. Geotech. Engrg. ASCE*, **101** (GT6), 551–569.

Craig R. F. (1987) *Soil Mechanics*, Chapman and Hall, 6th Edition.

Głębowicz K. (2006) Hypoplastic modelling of pre-failure behaviour of sand against experimental data, *Arch. of Hydro-Engineering and Environ. Mech.*, **53** (1), 31–47.

Kolymbas D. (2000) *Introduction to Hypoplasticity*, Balkema, Rotterdam/Brookfield.

Menzies B. K. (1988) A Computer Controlled Hydraulic Triaxial Testing System, *ASTM*, **977**, 82–94.

Poulos S. J. (1981) The steady state of deformation, *J. Geotech. Engrg. Div. ASCE,* **107** (GT5), 553–562.

Saada A. and Bianchini G. (eds.) (1987) Constitutive equations for granular non-cohesive soils, *Proc. of Int. Workshop,* Cleveland.

Sawicki A. (2003) Cam-clay approach to modelling pre-failure behaviour of sand against experimental data, *Arch. of Hydro-Engineering and Environ. Mech.*, **50** (3), 239–249.

Sawicki A. (2007) A study of pre-failure deformation of granular soils, *Arch. of Hydro-Engineering and Environ. Mech.*, **54** (3), 183–206.

Świdziński W. (2006) *Compaction-Liquefaction Mechanisms of Granular Soils*, in Polish, IBW PAN, Gdańsk.

Świdziński W. and Mierczyński J. (2002) On the measurement of axial strains in the triaxial test, *Arch. of Hydro-Engineering and Environ. Mech.*, **49** (1), 23–41.

Świdziński W. and Mierczyński J. (2005) Instability line as a basic characteristics of non-cohesive soils, *Arch. of Hydro-Engineering and Environ. Mech.,* **52** (1), 59–85.

Życzkowski M. (1973) *Complex Loads in Plasticity Theory*, PWN, Warszawa (in Polish).